

JHC *exPRESS*

Online publication date August 22, 2005

This article may be cited as DOI: 10.1369/jhc.5A6739.2005

Running headline: VMAT2 in hematopoietic cells and mastocytosis

**Vesicular monoamine transporter 2 (VMAT2) expression in hematopoietic cells
and in patients with systemic mastocytosis**

Martin Anlauf^{1,2}, Martin K.-H. Schäfer², Thorsten Schwark³, Nicole von Wurmb-Schwark³, Viktoria Brand¹, Bence Sipos¹, Hans-Peter Horny⁴, Reza Parwaresch⁵, Wolfgang Hartschuh⁶, Lee E. Eiden⁷, Günter Klöppel¹, Eberhard Weihe²

¹Dept. of Pathology, University of Kiel, Germany

²Dept. of Molecular Neuroscience, Institute of Anatomy and Cell Biology, University of Marburg, Germany

³Dept. of Anatomy and Dept. of Forensic Medicine, University of Kiel, Germany

⁴Dept. of Pathology, University of Lübeck, Germany

⁵Dept. of Hematopathology, University of Kiel, Germany

⁶Dept. of Dermatology, University of Heidelberg, Germany

⁷Section on Molecular Neuroscience, Laboratory of Cellular and Molecular Regulation, NIMH, Bethesda, MD, USA

Correspondence to:

Martin Anlauf, MD
Department of Pathology
University of Kiel
Michaelisstr. 11
24105 Kiel
Germany
Tel +49 431 597 3405
Fax +49 431 597 3462
E-mail: manlauf@path.uni-kiel.de

Supported by the Volkswagen-Stiftung, Germany, and the University of Kiel, Germany (F 344101).

Received for publication May 21, 2005; accepted August 1, 2005 [DOI:

10.1369/jhc.5A6739.2005].

Abstract

Uptake of monoamines into secretory granules is mediated by the vesicular monoamine transporters VMAT1 and VMAT2. In this study we analyzed their expression in inflammatory and hemotopoietic cells and in patients suffering from systemic mastocytosis (SM) and chronic myelogenous leukemia (CML). Normal human and monkey tissue specimens and tissues from patients suffering from SM and CML were analyzed by means of immunohistochemistry, radioactive *in situ* hybridization, real time RT-PCR, double fluorescence confocal laser scanning microscopy and immunoelectron microscopy. In normal tissue specimens, VMAT2, but not VMAT1, was expressed in mast cells, megakaryocytes, thrombocytes, basophil granulocytes and cutaneous Langerhans cells. Further hematopoietic and lymphoid cells showed no expression of VMATs. VMAT2 was expressed in all types of SM, as indicated by coexpression with the mast cell marker tryptase. In CML VMAT2 expression was retained in neoplastic megakaryocytes and basophil granulocytes. In conclusion, the identification of VMAT2 in mast cells, megakaryocytes, thrombocytes, basophil granulocytes and cutaneous Langerhans cells provides evidence that these cells possess molecular mechanisms for monoamine storage and handling. VMAT2 identifies normal and neoplastic mast cells, megakaryocytes and basophil granulocytes and may therefore become a valuable tool for the diagnosis of mastocytosis and malignant systemic diseases involving megakaryocytes and basophil granulocytes.

Key words: chronic myeloproliferative disease, histamine, mast cell, mastocytosis, tryptase, vesicular monoamine transporter

Introduction

Monoamines play an important role as neurotransmitters or hormones in the central and peripheral nervous system as well as in the endocrine and immune system. Their function depends on the location of the cells where they are synthesized, stored and released. All these monoamine-handling cells are characterized by the expression of proteins that enable them to store and secrete monoamines, such as plasma membrane transporters for scavenging and recycling monoamines from the extracellular space and intracellular transporters for monoamine storage (Weihe et al. 2000; Eiden 2000; Parsons 2000; Eiden et al. 2002). The uptake of monoamines from the cytoplasm into secretory granules is mediated by vesicular monoamine transporters (VMATs) along an ATPase-generated proton gradient (Schuldiner et al. 1995; Erickson et al. 1996; Erickson et al. 2000; Weihe et al. 2000; Eiden 2000; Travis et al. 2000). Two isoforms of the vesicular monoamine transporter were isolated from rat and human tissue and mapped to chromosome 8p21.3 (VMAT1) and chromosome 10q25 (VMAT2) (Erickson et al. 1992; Liu et al. 1992; Erickson et al. 1993; Peter et al. 1993). Their pharmacological profiles and their affinities for various monoamines such as catecholamines, histamine and serotonin have been analyzed in detail (Erickson et al. 1995; Erickson et al. 1996; Peter et al. 1996; Fon et al. 1997; Uhl et al. 2000).

VMAT1 and VMAT2 were found to be differentially expressed in monoamine-handling neurons of the central and peripheral nervous system (Weihe et al. 1994; Peter et al. 1995; Nirenberg et al. 1995; Schütz et al. 1998; Weihe et al. 2000; Anlauf et al. 2003b; Berkley et al. 2004), enterochromaffin- and enterochromaffin-like cells of the gastrointestinal tract (Weihe et al. 1994; Peter et al. 1995; Eissele et al. 1999; Weihe et al. 2000), and pancreatic beta-cells (Anlauf et al. 2003a). A few studies have shown that VMAT1 and VMAT2 serve as excellent markers for monoamine-handling tumors originating from monoaminergic cells of the gastroenteropancreatic system (GEP), the adrenal medulla and the paraganglia (Eissele et al. 1999; Rindi et al. 2000; Jakobsen et al. 2001; Anlauf et al. 2003a; Nilsson et al. 2004). In addition, specific radioligands have been developed and utilized for in vivo positron emission tomography to diagnose degenerative diseases of the CNS and neoplastic monoamine-handling endocrine cells of the GEP

This article may be cited as DOI: 10.1369/jhc.5A6739.2005 (Kilbourn 1997; Efang 2000; Frey et al. 2001; Kolby et al. 2001; Fuente-Fernandez et al. 2003; Kolby et al. 2003).

VMAT2 was originally cloned from a rat basophilic leukemia cell line (Erickson et al. 1992). This suggested that monoamine storage in this cell type is mediated by VMAT2. However, so far neither the *in vivo* expression of VMAT1 and VMAT2 in cells of the hematopoietic and lymphoid system nor their possible role as markers for myeloproliferative disorders has been examined in detail. Recently we found VMAT2 to be expressed in mast cells and cutaneous Langerhans cells of the skin (Anlauf et al. 2004). Our present study addressed three main issues: (1) do the extradermal mast cell also express VMAT2?, (2) are there other cells of the bone marrow that are positive for VMAT1 or VMAT2?, (3) are VMATs possible diagnostic tools for mastocytosis and for chronic myelogenous leukemia (CML), as representatives of myeloproliferative disorders?. In order to answer these questions we analyzed a series of different normal human and monkey tissues and specimens from patients suffering from mastocytosis and CML.

Material and Methods

Normal tissue specimens

Normal human tissue samples from various skin regions (n=10), the salivary glands, gastrointestinal tract and greater omentum (n=15), pancreas (n=5), liver, gallbladder and bile duct system (n=10), spleen (n=5), lymph nodes (n=10), tonsils (n=10), thymus (n=3), bone marrow (n=20), nose, trachea and lung (n=7), kidney and ureter (n=5), testis and prostate (n=5), uterus, tube and ovaries (n=5), heart and large blood vessels (n=5), thyroid gland and pituitary (n=5), various regions of the central nervous system (n=5), autonomous and spinal cord ganglia (n=5) and peripheral nerves (n=3) were used to analyze the expression of VMAT1 and VMAT2. Tissue samples similar in anatomic localization to those of humans were obtained from five rhesus monkeys, as described previously (Rausch et al. 1994). In addition, representative blood and bone marrow smears and buffy-coat-derived pooled platelets concentrates were analyzed. As positive control for VMAT1 and VMAT2 adrenal gland tissues from 2 rhesus monkeys and from 2 patients with unilateral adrenalectomy, one suffering from pheochromocytoma (m/63) and one from Conn's syndrome (w/70), were used.

For immunohistochemical analysis the human tissues were fixed in either Bouin-Hollande fixative, 10% formalin or 4% formaldehyde/PBS for 24-48 hours and then embedded in paraffin. The monkey tissues were perfused with 4% formaldehyde/PBS prior to postfixation in Bouin-Hollande for 24-48 hours, as described previously (Rausch et al. 1994). After dehydration in a graded series of 2-propanol solution, the tissues were embedded in Paraplast Plus (Merck, Darmstadt, Germany). Adjacent sections (3 µm or 5 µm thick) were cut and deparaffinized. Antigen retrieval to increase the sensitivity of immunodetection was performed by heating the sections at 92°-95° C for 15 min in 0.01 M citrate buffer (pH 6) according to the DAKO protocol (Hamburg, Germany). Non-specific binding sites were blocked with 5% bovine serum albumin (BSA, Serva, Heidelberg, Germany) in PBS (pH 7.45) followed by an avidin-biotin blocking step (avidin-biotin blocking kit, Boehringer Ingelheim, Germany).

For *in situ* hybridization human and monkey tissue specimens were immediately frozen in dry ice and stored at -80°C. Cryosections (12-16 µm thick)

were placed on pre-silanized glass slides, fixed in 4% phosphate-buffered formaldehyde for 60 min, followed by three 10 min washes in 50 mM PBS (pH 7.4). The slides were then briefly rinsed in distilled water, incubated in 0.1 M triethanolamine (pH 8.0) for 1 min and for 10 min in the same solution containing 0.25% v/v acetic anhydride under rapid stirring. They were then quickly rinsed in 2x SSC, dehydrated in 50 and 70% ethanol, and air dried.

Immunohistochemistry

Rabbit antiserum VMAT1/10 raised against the C-terminal sequence of human VMAT1 and antiserum no. 80182 raised against the C-terminal sequence of human VMAT2 were employed for the immunohistochemical investigations (Table 1). Post-staining with Giemsa and the antiserum against tryptase were used to identify mast cells of all organs (Horny et al. 1998). The CD25 antibody was used to discriminate between normal and neoplastic mast cells in patients with systemic mastocytosis (Sotlar et al. 2004). Further previously very well characterized antibodies were used to analyze the cell-specific expression of VMATs in bone marrow, lymph node, tonsil and thymus as summarized in Table 1.

The tissue sections were incubated with the primary antibodies overnight at 18°C (diluted as shown in Table 1) followed by a 2 h incubation at 37°C. The sections were then washed in distilled water and in 50 mM PBS and incubated with species-specific biotinylated secondary antibodies (Dianova, Hamburg, Germany) for 45 min at 37°C, washed several times and incubated for 30 min with the ABC reagents (Vectastatin Elite ABC kit, Boehringer Ingelheim, Germany). Immunoreactions with polyclonal antibodies were visualized with 3'-diaminobenzidine or enhanced by the addition of 0.08% ammonium nickel sulfate, as previously described (Anlauf et al. 2003a). Monoclonal antibodies were visualized by using an alkaline phosphatase system, as described previously (Kreipe et al. 1993).

The specificity of the immunohistochemical detection of VMAT1 and VMAT2 was analyzed by preabsorbing the antisera with 25 µM of the C-terminal human VMAT1 and VMAT2 peptide, respectively.

Generation of ³⁵S-labelled riboprobes

To generate specific radioactive cRNA probes for the detection of VMAT1 mRNA, a 247 bp-long DNA restriction fragment of hVMAT1 cDNA corresponding to nt. 436-682 was subcloned into Bluescript II KS+ (Stratagene, Heidelberg, Germany) (Erickson et al. 1996). For VMAT2 mRNA detection a 269 bp-long DNA fragment of hVMAT2 corresponding to nt. 244-512 was subcloned into pCDNAI (Invitrogen, Leek, the Netherlands) (Erickson et al. 1993). The inserted sequences were verified by double-stranded DNA sequencing. In vitro transcription of the two vector constructs using ³⁵S-UTP-labeled nucleotide yielded anti-sense riboprobes for hVMAT1 after linearization with XhoI and incubation with T7 RNA polymerase, and for hVMAT2 after linearization with XbaI and incubation with SP6 RNA polymerase. To increase the tissue penetration of the probes, the generated transcripts were reduced to about 200 nucleotide fragments by limited alkaline hydrolysis, as described previously (Angerer et al. 1987).

Radioactive *in situ* hybridization

To each section hybridization buffer (3xSSC, 50 mM NaPO₄, pH 7.4, 1x Denhardt's solution, 0.25 mg/ml yeast tRNA, 10% dextran sulfate, 50% formamide, 10 mM dithiothreitol) was applied. The hybridization mix contained 50,000 dpm/ml of ³⁵S-labeled RNA probes. The sections were coverslipped and incubated in moist chambers at 60° C for 16 h. The coverslips were then removed in 2xSSC and the sections were subjected to the following post-hybridization steps: RNase treatment (20 µg/ml RNase A and 1 U/ml RNase T1 in 10 mM Tris, pH 8.0, 0.5 M NaCl, 1 mM EDTA) for 60 min at 37° C and successive washes in decreasing salt concentrations (2x, 1x, 0.5x, and 0.2x SSC) for 10 min each, followed by incubation in 0.2x SSC at 60° C for 60 min.

For autoradiography the slides were dipped in NTB-2 nuclear emulsion (Eastman Kodak, Rochester, NY, USA) and developed after 3 weeks of exposure time. The developed sections were stained with hematoxylin and eosin, analyzed and photographed in dark-field and bright-field modus with an AX 70 microscope (Olympus, Hamburg, Germany).

RNA extraction and real time RT-PCR

From each cryo-protected normal human tissue specimen ten sections (10 μm thick) were cut and the first section was stained with hematoxylin and eosin. The other sections were used for dissection using a 24-gauge needle or a razor blade. Total RNA was extracted using Trizol according to the manufacturer's recommendations (Invitrogen, Karlsruhe, Germany). Equal amounts of RNA from each sample were reverse transcribed using random hexamer primers (Amersham Biosciences, Freiburg, Germany), and the cDNAs were used as templates in subsequent quantitative PCR reactions. Real time PCR was performed on an ABI Prism 7000 Sequence Detection System using commercially available specific primers and probes for the target, VMAT2, and the endogenous control, eukaryotic 18s rRNA (assays-on demand Hs00161858_m1, and Hs99999901_s1, respectively), and reagents as recommended by the manufacturer (all Applied Biosciences, Darmstadt, Germany). The relative levels of gene expression were calculated using the $\Delta\Delta C_t$ method as described by Cho et al. (Cho et al. 2003).

Confocal laser scanning microscopy

Double immunofluorescence was performed by covering the sections with a mixture of the two different primary antibodies in appropriate working dilutions (Table 1) and by subsequent labeling with the species-specific secondary antibodies coupled to the Alexa fluorochromes A647, A594, or A488 (MoBiTec, Göttingen, Germany) or the fluorochromes Cy2 or Cy3 (Dianova, Hamburg, Germany). Streptavidin coupled to Alexa fluorochromes A647, A488, or A594 (MoBiTec, Göttingen, Germany) or to Cy2 or to Cy3 was used in combination with biotinylated species-specific secondary antisera bearing the appropriate fluorochrome. For conventional double immunofluorescence, the sections were analyzed and photographed with an AX 70 microscope (Olympus, Hamburg, Germany) equipped with the appropriate filter cubes for discriminating between the different fluorochromes. Confocal double immunofluorescence analysis was performed with a Fluoview laser scanning microscope (Olympus). Digital confocal images were presented in false color.

Immunoelectron microscopy

Ultrathin sections were incubated overnight at room temperature with the polyclonal antibody against VMAT2 (1:1000) as previously described (Anlauf et al. 2000). After six 5 min rinses in PBS, pH 7.6, anti-rabbit goat IgG conjugated with 10 nm gold particles (Dianova, Hamburg, Germany) was applied at a dilution of 1:30. After a further incubation period of 90 min, the sections were rinsed with distilled water and contrasted with uranyl acetate and lead citrate (Weihe et al. 1991). Controls were performed by preabsorbing the antisera with 25 μ M of the C-terminal human VMAT2 peptide, respectively (Weihe et al. 1991). The sections were analyzed with a Philipps EM 400 electron microscope (Eindhoven, the Netherlands).

Tissue from patients with mastocytosis or CML

Formalin fixed tissue specimens from 31 patients suffering from systemic mastocytosis (SM) were retrieved from the consultation files of the Department of Pathology of the University of Lübeck and the Department of Hematopathology of the University of Kiel. In all of the patients with SM the neoplastic character of the mast cells had been confirmed on the basis of their CD25 expression, elevated tryptase serum levels and evident c-kit mutation D816V (Sotlar et al. 2004). The diagnoses followed the WHO classification system for mastocytosis (Valent et al. 2001b): indolent systemic mastocytosis (ISM, n=11), systemic mastocytosis with associated clonal hematological non-mast cell lineage disease (SM-AHNMD, n=11), aggressive systemic mastocytosis (ASM, n=6), mast cell leukemia (MCL; n=2), mast cell sarcoma (MCS, n=1). In 9 additional patients with typical clinical signs of cutaneous mastocytosis skin and bone marrow specimens were analyzed prospectively to confirm the clinical diagnosis and to determine whether or not they showed systemic involvement. To study the expression of VMAT1 and VMAT2 in CML, biopsies and smears from the bone marrow from 15 patients diagnosed according to the WHO criteria were obtained (Vardiman et al. 2001).

Ethics

The procurement of human material during surgery was approved by the Ethics Committees of the Medical Faculties of the University of Marburg and the Universities of Kiel and Lübeck. Oral informed consent was obtained from each

This article may be cited as DOI: 10.1369/jhc.5A6739.2005
patient prior to surgery. Monkey tissues were obtained in accordance with the
approved animal care and use protocols of Bioqual, Inc. (Rockville, MD, USA).

Results

Analysis of VMAT2 protein and mRNA expression in normal tissue specimens

Immunohistochemistry and radioactive *in situ* hybridization revealed an identical distribution pattern for VMAT2 protein and mRNA in a sizeable subpopulation of connective tissue- and mucosa-associated inflammatory cells (Figs. 1 and 2). In paraffin-embedded sections, the VMAT2-positive cells measured 8-15 μm in diameter, were round, oval or fusiform in shape and revealed granular cytoplasmic VMAT2 immunoreactivity, suggesting that these cells are mast cells (Fig. 1 B).

Real time RT-PCR analysis revealed VMAT2 mRNA in all tissues observed. It was most abundant in the skin, spleen, lung and the uterine cervix. Lower levels were found in the esophagus, the large and small intestine and the lymph nodes (Fig. 3).

The results of immunohistochemistry and *in situ* hybridization corresponded to each other. The highest density of VMAT2-positive cells was seen in the dermis, the lung, the tonsil and the spleen. In the dermal layer of the skin, the number of VMAT2-positive cells varied in different parts of the body, being most abundant in the scrotum and the prepuce of the penis. VMAT2 was also expressed in cutaneous Langerhans cells, as previously reported by our group (Anlauf et al. 2004) (data not shown).

All parts of the gut contained a sizeable subpopulation of VMAT2-positive cells in the lamina propria mucosae and in the connective tissue of the outer layers and the omenta (Figs. 1, 2 and 4 B). Scattered VMAT2-positive cells were seen along the ducts of the salivary glands and the pancreas and within the connective tissue of the bile duct system, but they were sparse in the acinar parenchyma. There were small numbers of VMAT2-positive cells in the portal tracts and sinusoids of the liver (data not shown).

In lymphoid organs and the bone marrow the highest densities of VMAT2-positive cells were seen in the peritonsillar connective tissue and in close association with fibrous septa of the tonsil and the spleen. The connective tissue of the thymus and the lymph nodes revealed scattered VMAT2-positive cells, but lymphocytes were VMAT2 negative (Fig. 4 A). In the bone marrow all megakaryocytes were VMAT2 positive (Fig. 4 D). In addition, a minor subpopulation

of less than 0.5% of the hematopoietic cells, mainly localized around the small blood vessels, were VMAT2-positive (Fig. 4 D).

High densities of VMAT2-positive cells were seen in all parts of the respiratory system. In the nose, the trachea and the bronchi some of these cells had migrated into the respiratory epithelium, while in the lung parenchyma most VMAT2-positive cells were localized within the connective tissue of the alveolar septa (Fig. 4 C).

In the nervous system VMAT2-positive cells were extremely sparse. They were found in close association with nerve cells of the autonomic ganglia and peripheral nerves and close to blood vessels of the CNS, with the highest densities being seen within the leptomeninges. In all other organs (heart and large blood vessels, urogenital tract and endocrine organs) VMAT2-positive cells were sparse. Most of them were localized within the connective tissue (data not shown).

Identification of the cellular phenotype of VMAT2-positive cells

In all lymphoid organs and in the lamina propria mucosae and the connective tissue of other organ systems VMAT2 was expressed in mast cells, as demonstrated by confocal laser scanning double fluorescence microscopy, which revealed full coexpression of VMAT2 and tryptase (Fig. 4 E-G). In contrast, VMAT1 was absent from inflammatory cells, but was expressed in some neuroendocrine cells of the epithelial layers. High resolution confocal laser scanning microscopy and immunoelectron microscopy showed that VMAT2 was localized at the membrane of the secretory granules of mast cells (Fig. 4 H-J and Fig. 5). Other inflammatory cells, including various maturation stages of B-lymphocytes and T-lymphocytes (CD 3, 4, 5, 8, 10, 15, 20, 23, 30, 79a and bcl2) and plasma cells (kappa, lambda, CD38, CD79a), were negative for VMAT2. With the exception of CD1a-positive Langerhans cells of the epidermal layer, macrophages and dendritic cells of all lymphoid organs did not reveal any immunoreactivity for VMAT1 and VMAT2 (data not shown).

In the hematopoietic system, VMAT2 was expressed in CD61-positive megakaryocytes and in thrombocytes (Fig. 4 D and 6). Further VMAT2 expressing cells of the bone marrow comprised less than 0.5% hematopoietic cells and were identified as mast cells (VMAT2+/tryptase+) and basophil granulocytes (VMAT2+/tryptase-). Other hematopoietic cells, e.g. CD34-positive cells, erythropoietic cells (glycophorin A), granulopoietic precursor cells (ki-My2) and

eosinophil granulocytes, which were identified by their typical granules, were negative for VMAT1 and VMAT2. (data not shown)

Expression of VMAT2 in patients with mastocytosis and CML

VMAT2 but not VMAT1 was found to be expressed in all patients with cutaneous and systemic mastocytosis, irrespective of the infiltration pattern, subtype of SM and granule content (Figs. 7 and 8). The number of VMAT2 positive mast cells almost equaled that of tryptase-immunoreactive cells (Fig. 8). The immunohistochemical detection of VMAT2 and tryptase was of equal diagnostic relevance, with the exception of two ASM cases that revealed reduced immunoreactivity for tryptase but strong VMAT2 expression (Fig. 8 D-G).

In bone marrow specimens from patients suffering from CML, VMAT2 expression was seen in all megakaryocytes, in particular in cases with extensive proliferation of small hypolobulated megakaryocytes. There was a slight increase in mast cells (VMAT2+/tryptase+) in most specimens. Basophilia (VMAT2+/tryptase-) identified in blood and bone marrow smears was present in all cases. VMAT2 was absent from all other neoplastic cell populations, e.g. neutrophils and eosinophils, and erythropoietic cells (data not shown).

Discussion

In a recent study we showed that the expression of VMAT2 characterizes cutaneous mast cells and epidermal Langerhans cells (Anlauf et al. 2004). We can extend this observation by showing that VMAT2 is expressed in mast cells from all human and monkey organs. In addition, VMAT2 but not VMAT1 was found to be expressed in megakaryocytes, thrombocytes and basophil granulocytes. Both VMAT2 and VMAT1 were absent from lymphocytes, plasma cells and neutrophil and eosinophil granulocytes, erythropoietic cells and, with the exception of cutaneous Langerhans cells, also from dendritic cells and macrophages. VMAT2 is expressed in all mast cells, megakaryocytes and basophil granulocytes, regardless of whether they are derived from patients or healthy controls.

It is well known that mast cells, which derive from CD34-positive bone marrow stem cells, store monoamines. Mediators of mast cells stored and released in granules, e.g. histamine, function as amplifiers of the inflammatory response (Kaliner 1979; Serafin et al. 1987; Kunzmann et al. 2003). Among the differential immunohistochemical markers for mast cells, tryptase is the most sensitive and ubiquitous (Horny et al. 1998). Our results showed, on the basis of its coexpression with tryptase, that VMAT2 is expressed in mast cells of all human and monkey organs. The immunohistochemical distribution pattern of VMAT2 matched the results of the radioactive *in situ* hybridization and RT-PCR. By using high resolution confocal laser scanning microscopy and immunoelectron microscopy we were able to localize VMAT2 to the membrane of secretory granules in mast cells. These observations, together with the previous pharmacological finding that VMAT2 knockout mice lack the capacity to release histamine and serotonin from mast cells (Travis et al. 2000), further supports the view that VMAT2 plays an active role in monoamine handling in mast cells of rodents and primates.

The expression of VMAT2 by megakaryocytes and basophil granulocytes indicates sequestration of monoamines in these cells. In contrast, absence of VMAT1 and VMAT2 from other cells of the hematopoietic and lymphoid lineage, e.g. eosinophil and neutrophil granulocytes, erythropoietic cells, lymphocytes and plasma cells, shows that vesicular monoamine storage mechanisms are restricted to megakaryocytes and basophil granulocytes. Though it has been suggested that

VMATs can be transcriptionally activated in a pre-B cell line and may be present in peripheral blood lymphocytes (Watson et al. 1999; Amenta et al. 2001), we could not confirm these observations *in situ*. While there is strong evidence in the literature that lymphocytes synthesize catecholamines (Bergquist et al. 1994; Josefsson et al. 1996; Musso et al. 1996), our results suggest that storage of monoamines in lymphocytes is not dependent on VMATs. On the other hand, it is well established that basophil granulocytes store histamine and megakaryocytes accumulate serotonin (Dvorak et al. 1995; Dvorak et al. 1996; Holtje et al. 2003). Our results showed that VMAT2 is responsible for the sequestration of monoamines in these cell types. The reported absence of VMAT2 from macrophages other than cutaneous Langerhans cells implies that macrophages obtain a monoamine-handling phenotype specifically when they have entered the epidermis. Langerhans cells seem to lose their VMAT2 phenotype during their migration to lymphoid organs.

Recently, VMATs were found to be excellent tools for the pathological and scintigraphic diagnosis of degenerative diseases of the CNS and certain neoplastic monoamine-handling endocrine cells of the GEP (Eissele et al. 1999; Jakobsen et al. 2001; Kolby et al. 2001; Kolby et al. 2003; Nilsson et al. 2004). Based on the observation that neoplastic mast cells retain their VMAT2 phenotype in cutaneous mastocytosis (Anlauf et al. 2004), we anticipated that VMAT2 might also serve as a marker for systemic mastocytosis, which is a persistent clonal disease of bone marrow-derived myelomastocytic progenitor cells and therefore differs from cutaneous mastocytosis (Valent et al. 2001a; Valent et al. 2004). The diagnosis of mastocytosis is traditionally based on the demonstration of focal accumulations of mast cells with typical histological and cytomorphological properties (Lennert et al. 1979; Horny et al. 2001; Valent et al. 2001a). However, depending on the organ system examined, type of mast cell disease and presence of other diseases, it is sometimes difficult to diagnose mastocytosis histologically (Horny et al. 1985; Horny et al. 1988; Horny et al. 1989; Horny et al. 1992). Our study demonstrated that VMAT2 can be used as an excellent pathological marker not only of cutaneous but also of systemic mastocytosis, comparable to the well established mast cell marker tryptase (Li et al. 1996; Horny et al. 1998).

CML is a myeloproliferative disease that originates from an abnormal pluripotent bone marrow stem cell. Most of the CML patients have increased

numbers of mast cells, basophil granulocytes and megakaryocytes (Vardiman et al. 2001). Our finding that VMAT2 expression is retained in these neoplastic cell types indicates that monoamine-storage mechanisms are conserved in this condition and that VMAT2 can be used as a marker to identify monoamine-handling cell populations. However, as VMAT2 is expressed in all mast cells, regardless of whether they are derived from patients or healthy controls, a distinction between normal mast cells and different subtypes of mastocytosis based on their VMAT2 expression patterns is not possible. So far it is not known whether VMAT2 is also expressed in hematological disorders other than mastocytosis and CML. It would be of interest to analyze in which maturation stages neoplastic hematopoietic cells in acute myeloid leukemia (AML) obtain monoaminergic properties, as it has been reported that some types of AML showed tryptase and CD117 expression as well as elevated serum levels of circulating tryptase (Sperr et al. 2001; Sperr et al. 2002). However, this should be the subject of a further study.

It has been mentioned that increased VMAT2 binding can be visualized in the normal tonsils and in the nasal lymphoid tissue by positron emission tomography (PET) (Meyer et al. 2000). Our findings provide the morphological substrate for this observation, namely the enrichment of VMAT2-positive mast cells in these regions. As we have shown in our study that VMAT2 is an excellent pathological marker for all types of mastocytoses and neoplastic monoamine handling cells, it should now be possible to develop PET imaging strategies for the diagnosis of mastocytosis and myeloproliferative disorders.

In conclusion, the selective expression of VMAT2, which is responsible for the uptake and accumulation of biogenic amines in secretory granules to make them available for exocytotic release, is a new important feature in the functional spectrum of mast cells, megakaryocytes and basophil granulocytes. VMAT2 is a useful diagnostic tool for identifying normal mast cells and neoplastic mast cells in all different subtypes of mastocytosis. The identification of VMAT2 in cells of the hematopoietic system provides evidence of a molecular mechanism for monoamine storage and handling in these cells, and provides a basis for imaging, as well as for promoting and interfering with monoamine loading of these cells in myeloproliferative diseases such as CML.

Acknowledgements

We would like to thank Maike Pacena, Anja Bredtmann, Tanja Hein, Heidi Hlavaty, Alice Johl, Heike Ristau, Elke Rodenberg-Frank, Petra Sack and Marion Zibuschka for their excellent technical assistance and Heidemarie Schneider and Waldemar Strauss for the brilliant photographic documentation. We are indebted to Katherine Dege for critically reading and editing the manuscript. We thank all colleagues who provided clinical data on the patients. Some of the results of this study are part of Viktoria Brand's MD thesis.

Literature Cited

Amenta F, Bronzetti E, Cantalamessa F, El Assouad D, Felici L, Ricci A, Tayebati SK (2001) Identification of dopamine plasma membrane and vesicular transporters in human peripheral blood lymphocytes. *J Neuroimmunol* 117:133-142

Angerer LM, Stoler MH, Angerer RC (1987) In situ hybridization with RNA-probes: an annotated recipe. In Valentino L, Eberwine I, Barchas D eds. *In situ hybridization: application to neurobiology*. New York, Oxford University Press, 42-70

Anlauf M, Eissele R, Schäfer MK, Eiden LE, Arnold R, Pauser U, Klöppel G, Weihe E (2003a) Expression of the two isoforms of the vesicular monoamine transporter (VMAT1 and VMAT2) in the endocrine pancreas and pancreatic endocrine tumors. *J Histochem Cytochem* 51:1027-1040

Anlauf M, Schäfer MK, Depboylu C, Hartschuh W, Eiden LE, Klöppel G, Weihe E (2004) The vesicular monoamine transporter 2 (VMAT2) is expressed by normal and tumor cutaneous mast cells and Langerhans cells of the skin but is absent from Langerhans cell histiocytosis. *J Histochem Cytochem* 52:779-788

Anlauf M, Schäfer MK, Eiden L, Weihe E (2003b) Chemical coding of the human gastrointestinal nervous system: cholinergic, VIPergic, and catecholaminergic phenotypes. *J Comp Neurol* 459:90-111

Anlauf M, Weihe E, Hartschuh W, Hamscher G, Feurle GE (2000) Localization of xenin-immunoreactive cells in the duodenal mucosa of humans and various mammals. *J Histochem Cytochem* 48:1617-1626

Berkley KJ, Dmitrieva N, Curtis KS, Papka RE (2004) Innervation of ectopic endometrium in a rat model of endometriosis. *Proc Natl Acad Sci USA* 101:11094-11098

Bergquist J, Tarkowski A, Ekman R, Ewing A (1994) Discovery of endogenous catecholamines in lymphocytes and evidence for catecholamine regulation of lymphocyte function via an autocrine loop. *Proc Natl Acad Sci* 91:12912-12916

Cho SH, Yao Z, Wang SW, Alban RF, Barbers RG, French SW, Oh CK (2003) Regulation of activin A expression in mast cells and asthma: its effect on the proliferation of human airway smooth muscle cells. *J Immunol* 170:4045-4052

Dvorak AM, MacGlashan DW, Jr., Morgan ES, Lichtenstein LM (1995) Histamine distribution in human basophil secretory granules undergoing FMLP-stimulated secretion and recovery. *Blood* 86:3560-3566

Dvorak AM, MacGlashan DW, Jr., Morgan ES, Lichtenstein LM (1996) Vesicular transport of histamine in stimulated human basophils. *Blood* 88:4090-4101

Efange SM (2000) In vivo imaging of the vesicular acetylcholine transporter and the vesicular monoamine transporter. *FASEB J* 14:2401-2413

Eiden LE (2000) The vesicular neurotransmitter transporters: current perspectives and future prospects. *FASEB J* 14:2396-2400

Eiden LE, Schütz B, Anlauf M, Depboylu C, Schäfer MKH, Weihe E (2002) The vesicular monoamine transporters (VMATs): role in the chemical coding of neuronal transmission and monoamine storage in amine-handling immune and inflammatory cells. In Nagatsu T, Nabeshima T, McCarty R, Goldstein DS eds. *Catecholamine research: from molecular insights to clinical medicine*. New York, Kluwer Academic/Plenum Publishers, 23-33

Eissele R, Anlauf M, Schäfer MKH, Eiden LE, Arnold R, Weihe E (1999) Expression of vesicular monoamine transporters in endocrine hyperplasia and endocrine tumors of the oxyntic stomach. *Digestion* 60:428-439

Erickson JD, Eiden LE (1993) Functional identification and molecular cloning of a human brain vesicle monoamine transporter. *J Neurochem* 61:2314-2317

Erickson JD, Eiden LE, Hoffman BJ (1992) Expression cloning of a reserpine-sensitive vesicular monoamine transporter. *Proc Natl Acad Sci USA* 89:10993-10997

Erickson JD, Eiden LE, Schäfer MK, Weihe E (1995) Reserpine- and tetrabenazine-sensitive transport of (3)H-histamine by the neuronal isoform of the vesicular monoamine transporter. *J Mol Neurosci* 6:277-287

Erickson JD, Schäfer MK, Bonner TI, Eiden LE, Weihe E (1996) Distinct pharmacological properties and distribution in neurons and endocrine cells of two isoforms of the human vesicular monoamine transporter. *Proc Natl Acad Sci USA* 93:5166-5171

Erickson JD Varoqui H (2000) Molecular analysis of vesicular amine transporter function and targeting to secretory organelles. *FASEB J* 14:2450-2458

Fon EA, Pothos EN, Sun BC, Killeen N, Sulzer D, Edwards RH (1997) Vesicular transport regulates monoamine storage and release but is not essential for amphetamine action. *Neuron* 19:1271-1283

Frey KA, Koeppe RA, Kilbourn MR (2001) Imaging the vesicular monoamine transporter. *Adv Neurol* 86:237-247

Fuente-Fernandez R, Furtado S, Guttman M, Furukawa Y, Lee CS, Calne DB, Ruth TJ, Stoessl AJ (2003) VMAT2 binding is elevated in dopa-responsive dystonia: visualizing empty vesicles by PET. *Synapse* 49:20-28

Holtje M, Winter S, Walther D, Pahner I, Hortnagl H, Ottersen OP, Bader M, Ahnert-Hilger G (2003) The vesicular monoamine content regulates VMAT2 activity through Galphaq in mouse platelets. Evidence for autoregulation of vesicular transmitter uptake. *J Biol Chem* 278:15850-15858

Horny HP Kaiserling E (1988) Lymphoid cells and tissue mast cells of bone marrow lesions in systemic mastocytosis: a histological and immunohistological study. *Br J Haematol* 69:449-455

Horny HP, Kaiserling E, Campbell M, Parwaresch MR, Lennert K (1989) Liver findings in generalized mastocytosis. A clinicopathologic study. *Cancer* 63:532-538

Horny HP, Parwaresch MR, Lennert K (1985) Bone marrow findings in systemic mastocytosis. *Hum Pathol* 16:808-814

Horny HP, Ruck MT, Kaiserling E (1992) Spleen findings in generalized mastocytosis. A clinicopathologic study. *Cancer* 70:459-468

Horny HP, Sillaber C, Menke D, Kaiserling E, Wehrmann M, Stehberger B, Chott A, Lechner K, Lennert K, Valent P (1998) Diagnostic value of immunostaining for tryptase in patients with mastocytosis. *Am J Surg Pathol* 22:1132-1140

Horny HP Valent P (2001) Diagnosis of mastocytosis: general histopathological aspects, morphological criteria, and immunohistochemical findings. *Leuk Res* 25:543-551

Jakobsen AM, Andersson P, Saglik G, Andersson E, Kolby L, Erickson JD, Forssell-Aronsson E, Wängberg B, Ahlman H, Nilsson O (2001) Differential expression of vesicular monoamine transporter (VMAT) 1 and 2 in gastrointestinal endocrine tumours. *J Pathol* 195:463-472

Josefsson E, Bergquist J, Ekman R, Tarkowski A (1996) Catecholamines are synthesized by mouse lymphocytes and regulate function of these cells by induction of apoptosis. *Immunology* 88:140-146

Kaliner MA (1979) The mast cell--a fascinating riddle. *N Engl J Med* 301:498-499

Kilbourn MR (1997) In vivo radiotracers for vesicular neurotransmitter transporters. *Nucl Med Biol* 24:615-619

Kolby L, Bernhardt P, Ahlman H, Wangberg B, Johanson V, Wigander A, Forssell-Aronsson E, Karlsson S, Ahren B, Stenman G, Nilsson O (2001) A transplantable human carcinoid as model for somatostatin receptor-mediated and amine transporter-mediated radionuclide uptake. *Am J Pathol* 158:745-755

Kolby L, Bernhardt P, Levin-Jakobsen AM, Johanson V, Wangberg B, Ahlman H, Forssell-Aronsson E, Nilsson O (2003) Uptake of meta-iodobenzylguanidine in neuroendocrine tumours is mediated by vesicular monoamine transporters. *Br J Cancer* 89:1383-1388

Kreipe H, Wacker HH, Heidebrecht HJ, Haas K, Hauberg M, Tiemann M, Parwaresch R (1993) Determination of the growth fraction in non-Hodgkin's lymphoma by monoclonal antibody Ki-S5 directed against a formalin-resistant epitope of the Ki-67 antigen. *Am J Pathol* 142:1689-1694

Kunzmann S, Mantel PY, Wohlfahrt JG, Akdis M, Blaser K, Schmidt-Weber CB (2003) Histamine enhances TGF-beta1-mediated suppression of Th2 responses. *FASEB J* 17:1089-1095

Lennert K, Parwaresch MR (1979) Mast cells and mast cell neoplasia: a review. *Histopathology* 3:349-365

Li WV, Kapadia SB, Sonmez-Alpan E, Swerdlow SH (1996) Immunohistochemical characterization of mast cell disease in paraffin sections using tryptase, CD68, myeloperoxidase, lysozyme, and CD20 antibodies. *Mod Pathol* 9:982-988

Liu Y, Peter D, Roghani A, Schuldiner S, Prive GG, Eisenberg D, Brecha N, Edwards RH (1992) A cDNA that suppresses MPP+ toxicity encodes a vesicular amine transporter. *Cell* 70:539-551

Meyer P, Bohnen NI, Steele JM, Koeppe RA, Anzai Y, Kuhl DE, Frey KA (2000) Increased VMAT2 binding in nasal associated lymphoid tissue (NALT) in Tourette syndrome studied with (+)-alpha-(11C)DTBZ PET. *J Nucl Med* 41 (Suppl.):26P-

Musso NR, Brenci S, Setti M, Indiveri F, Lotti G (1996) Catecholamine content and in vitro catecholamine synthesis in peripheral human lymphocytes. *J Clin Endocrinol Metab* 81:3553-3557

Nilsson O, Jakobsen AM, Kolby L, Bernhardt P, Forssell-Aronsson E, Ahlman H (2004) Importance of vesicle proteins in the diagnosis and treatment of neuroendocrine tumors. *Ann N Y Acad Sci* 1014:280-283

Nirenberg MJ, Liu Y, Peter D, Edwards RH, Pickel VM (1995) The vesicular monoamine transporter 2 is present in small synaptic vesicles and preferentially localizes to large dense core vesicles in rat solitary tract nuclei. *Proc Natl Acad Sci USA* 92:8773-8777

Parsons SM (2000) Transport mechanisms in acetylcholine and monoamine storage. *FASEB J* 14:2423-2434

Peter D, Finn JP, Klisak I, Liu Y, Kojis T, Heinzmann C, Roghani A, Sparkes RS, Edwards RH (1993) Chromosomal localization of the human vesicular amine transporter genes. *Genomics* 18:720-723

Peter D, Liu Y, Sternini C, De Giorgio R, Brecha N, Edwards RH (1995) Differential expression of two vesicular monoamine transporters. *J Neurosci* 15:6179-6188

Peter D, Vu T, Edwards RH (1996) Chimeric vesicular monoamine transporters identify structural domains that influence substrate affinity and sensitivity to tetrabenazine. *J Biol Chem* 271:2979-2986

Rausch DM, Heyes MP, Murray EA, Lendvay J, Sharer LR, Ward JM, Rehm S, Nohr D, Weihe E, Eiden LE (1994) Cytopathologic and neurochemical correlates of progression to motor/cognitive impairment in SIV-infected rhesus monkeys. *J Neuropathol Exp Neurol* 53:165-175

Rindi G, Paolotti D, Fiocca R, Wiedenmann B, Henry JP, Solcia E (2000) Vesicular monoamine transporter 2 as a marker of gastric enterochromaffin-like cell tumors.

Virchows Arch 436:217-223

Schuldiner S, Shirvan A, Linial M (1995) Vesicular neurotransmitter transporters: from bacteria to humans. *Physiol Rev* 75:369-392

Schütz B, Schäfer MKH, Eiden LE, Weihe E (1998) Vesicular amine transporter expression and isoform selection in developing brain, peripheral nervous system and gut. *Brain Res Dev Brain Res* 106:181-204

Serafin WE Austen KF (1987) Mediators of immediate hypersensitivity reactions. *N Engl J Med* 317:30-34

Sotlar K, Horny HP, Simonitsch I, Krokowski M, Aichberger KJ, Mayerhofer M, Printz D, Fritsch G, Valent P (2004) CD25 indicates the neoplastic phenotype of mast cells: a novel immunohistochemical marker for the diagnosis of systemic mastocytosis (SM) in routinely processed bone marrow biopsy specimens. *Am J Surg Pathol* 28:1319-1325

Sperr WR, Hauswirth AW, Valent P (2002) Tryptase a novel biochemical marker of acute myeloid leukemia. *Leuk Lymphoma* 43:2257-2261

Sperr WR, Jordan JH, Baghestanian M, Kiener HP, Samorapoompichit P, Semper H, Hauswirth A, Schernthaner GH, Chott A, Natter S, Kraft D, Valenta R, Schwartz LB, Geissler K, Lechner K, Valent P (2001) Expression of mast cell tryptase by myeloblasts in a group of patients with acute myeloid leukemia. *Blood* 98:2200-2209

Travis ER, Wang YM, Michael DJ, Caron MG, Wightman RM (2000) Differential quantal release of histamine and 5-hydroxytryptamine from mast cells of vesicular monoamine transporter 2 knockout mice. *Proc Natl Acad Sci USA* 97:162-167

Uhl GR, Li S, Takahashi N, Itokawa K, Lin Z, Hazama M, Sora I (2000) The VMAT2 gene in mice and humans: amphetamine responses, locomotion, cardiac arrhythmias, aging, and vulnerability to dopaminergic toxins. *FASEB J* 14:2459-2465

Valent P, Horny HP, Escribano L, Longley BJ, Li CY, Schwartz LB, Marone G, Nunez R, Akin C, Sotlar K, Sperr WR, Wolff K, Brunning RD, Parwaresch RM, Austen KF, Lennert K, Metcalfe DD, Vardiman JW, Bennett JM (2001a) Diagnostic criteria and classification of mastocytosis: a consensus proposal. *Leuk Res* 25:603-625

Valent P, Horny HP, Li CY, Longley BJ, Metcalfe DD, Parwaresch RM, Bennett JM (2001b) Mastocytosis. In Jaffe ES, Harris NL, Stein H, Vardiman JW eds. *Pathology and genetics. Tumours of haematopoietic and lymphoid tissues. WHO Classification of Tumours*. Lyon, IARC Press, 293-302

Valent P, Sperr WR, Schwartz LB, Horny HP (2004) Diagnosis and classification of mast cell proliferative disorders: delineation from immunologic diseases and non-mast cell hematopoietic neoplasms. *J Allergy Clin Immunol* 114:3-11

Vardiman JW, Pierre R, Thiele J, Imbert M, Brunning RD, Flandrin G (2001) Chronic myelogenous leukaemia. In Jaffe ES, Harris NL, Stein H, Vardiman JW eds. *Pathology and genetics. Tumours of haematopoietic and lymphoid tissues. WHO Classification of Tumours*. Lyon, IARC Press, 20-26

Watson F, Deavall DG, Macro JA, Kiernan R, Dimaline R (1999) Transcriptional activation of vesicular monoamine transporter 2 in the pre-B cell line Ea3.123. *Biochem J* 337 (Pt 2):193-199

Weihe E Eiden LE (2000) Chemical neuroanatomy of the vesicular amine transporters. *FASEB J* 14:2435-2449

Weihe E, Hartschuh W, Nohr D (1991) Light microscopic immunoenzyme and electron microscopic immunogold cytochemistry reveal tachykinin immunoreactivity in Merkel cells of pig skin. *Neurosci Lett* 124:260-263

Weihe E, Schäfer MKH, Erickson JD, Eiden LE (1994) Localization of vesicular monoamine transporter isoforms (VMAT1 and VMAT2) to endocrine cells and neurons in rat. *J Mol Neurosci* 5:149-164

Table 1. List of primary antibodies

Antigen ^a	Clone/Code	Source/Reference	Dilution ^b	Species ^c
VMAT1	VMAT1/10	Erickson et al. 1996	1:4000/1:300(f) ^a	rabbit polycl.
VMAT2	80182	Erickson et al. 1996	1:4000/1:400(f)	rabbit polycl.
bcl2	bcl2-100	Zymed Lab, San Francisco, USA	1:50	mouse monocl.
CD1a	010	DAKO, Glostrup, Denmark	1:50/1:5(f)	mouse monocl.
CD3	NCI-CD3-PS1	Novocastra, Newcastle, UK	1:20	mouse monocl.
CD4	NCI-CD4-1F6	Novocastra, Newcastle, UK	1:10	mouse monocl.
CD5	NCI-CD5-4C7	Novocastra, Newcastle, UK	1:25	mouse monocl.
CD8	144B	DAKO, Glostrup, Denmark	1:50	mouse monocl.
CD10	NCI-CD10-270	Novocastra, Newcastle, UK	1:10	mouse monocl.
CD15	C3D-1	DAKO, Glostrup, Denmark	1:20	mouse monocl.
CD20	JHM1A9/5	R. Parwaresch, Kiel, Germany	1:10	mouse monocl.
CD23	NCI-CD23-1B12	Novocastra, Newcastle, UK	1:40	mouse monocl.
CD30	BerH2	R. Parwaresch, Kiel, Germany	1:1	mouse monocl.
CD34	1185	Immunotech, Marseille, France	1:1	mouse monocl.
CD38	NCL-CD38-290	Novocastra, Newcastle, UK	1:100	mouse monocl.
CD61	Y2-51	DAKO, Glostrup, Denmark	1:25	mouse monocl.
CD79a	JCB117	DAKO, Glostrup, Denmark	1:200	mouse monocl.
Glycophorin A	JC159	DAKO, Glostrup, Denmark	1:50	mouse monocl.
Kappa	A0191	DAKO, Glostrup, Denmark	1:5000	rabbit polycl.
Ki-M1P	IV20	R. Parwaresch, Kiel, Germany	1:10	mouse monocl.
Ki-My2	B2C164	R. Parwaresch, Kiel, Germany	1:10	mouse monocl.
Lambda	A0193	DAKO, Glostrup, Denmark	1:5000	rabbit polycl.
S100	Z0311	DAKO, Glostrup, Denmark	1:5000	rabbit polycl.
Tryptase	AA1	DAKO, Glostrup, Denmark	1:30,000/1:2000(f)	mouse monocl.

^aVMAT1/2, vesicular monoamine transporter; HDC, histidine decarboxylase;

^b(f), dilution for immunofluorescence; ^cmonocl., monoclonal; polycl., polyclonal

Legends

Figure 1. Expression of VMAT2 in the connective tissue of the gut

(A-D) Immunohistochemistry, paraffin-embedded sections. Low power bright-field magnification of the outer smooth muscle layers of the stomach revealing scattered VMAT2-positive cells (arrows in A) as well as some VMAT2-positive nerve fibers (A). The high power magnification (inset B) shows a morphology typical for mast cells. The VMAT2 immunostaining in an adjacent section is completely abolished after preincubation of the VMAT2 antiserum with 25 μ M VMAT2 peptide (C). VMAT1 is absent from cells and from nerve fibers (D).

(E-G) Radioactive *in situ* hybridization, cryosections. Low power dark-field magnification of the outer smooth muscle layers of the stomach revealing a similar pattern of VMAT2 mRNA expression (arrows in E; VMAT2 antisense probe). These scattered cells are negative for the VMAT2 sense control (F) and for the VMAT1 antisense probe (G).

Scale bars = 200 μ m in A, C, D, 5 μ m in B, 100 μ m in E, F, G

Figure 2. Expression of VMAT2 in the mucosa and submucosa of the gut

(A-C) Immunohistochemistry, paraffin-embedded sections. High power brightfield magnification of duodenal villus revealing scattered VMAT2-positive cells within the lamina propria layer (arrowheads in A). VMAT2 immunostaining in an adjacent section is completely abolished after preincubation of the VMAT2 antiserum with 25 μ M VMAT2 peptide (B). VMAT1 is absent from immune cells of the lamina propria but is present in endocrine cells within the epithelial layer (arrowheads in C).

(D) Radioactive *in situ* hybridization, cryosections. High power bright-field magnification of duodenal villi exhibiting a similar expression pattern of VMAT2 mRNA in the lamina propria (arrowheads). VMAT2 mRNA is absent from the epithelial layer. The high power magnification inset (E) shows dense perinuclear VMAT2 signals in such a lamina propria cell.

(F-G) Immunohistochemistry and *in situ* hybridization showing a corresponding distribution pattern of VMAT2 protein (F) and mRNA (G) in scattered immune cells (arrowheads in F and G) around submucosal blood vessels.

Scale bars = 100 μm in A – C, 20 μm in D, 5 μm in E, F, G, 20 μm in F, G

Figure 3. Detection of VMAT2 mRNA in various tissue specimens by real time RT-PCR

The diagram shows the difference in VMAT2 expression in the respective tissues in comparison with a skin specimen from the trunk, which was defined as standard and has a relative value of 1. Significant amounts of VMAT2 mRNA were detected in all tissues investigated, with the expression level ranging from 0.02 (diaphragm) to 4.29 (lung).

Figure 4. Expression of VMAT2 in various lymphoid tissues and the bone marrow

(A-D) Immunohistochemistry for VMAT2 in the tonsil (A), mucosa of the large intestine (B), the alveolar parenchyma of the lung (C) and the bone marrow (D). Scattered immune cells in all lymphoid tissues strongly express VMAT2 (A-C). Megakaryocytes and a minor population of cells showing round to oval nuclei and granular appearance representing mast cells and basophils showing VMAT2 expression (D).

(E-G) Confocal laser scanning double fluorescence microscopy for VMAT2 (green in E) and tryptase (red in F) demonstrating a high density of VMAT2- and tryptase-positive cells within the fibrous septa of the tonsil. The yellow color in composite image G demonstrates full coexpression of VMAT2 and tryptase in those cells.

(H-J) VMAT2 (green in H) and tryptase (red in I) showing colocalization in most secretory granules of a single mast cell (indicated by the yellow color in composite J). Note that VMAT2 is localized at the periphery of granules, while tryptase accumulated within the secretory vesicles.

Scale bars = 100 μm in A, B, 80 μm in C, 40 μm in D, 20 μm in E - G, 5 μm in H - K

Figure 5. Subcellular localization of VMAT2 in the mast cell

Immunoelectron microscopic localization of VMAT2 protein to secretory granules of a cutaneous mast cell. Gold particles representing the VMAT2 immunogold precipitate are closely associated with the membrane of secretory granules within a mast cell.

Scale bar = 150 nm

Figure 6. Expression of VMAT2 in thrombocytes

Confocal laser scanning double fluorescence microscopy for VMAT2 (green) showing a granular immunoreactivity of thrombocytes (pooled platelet concentrate).

Scale bar = 150 μ m

Figure 7. Expression of VMAT2 in patients with cutaneous mastocytosis

(A, B) Radioactive *in situ* hybridization, cryosections. High power dark-field magnification demonstrating strong VMAT2 mRNA expression in a subepidermal mast cell infiltrate (A, VMAT2 antisense). Hybridization with the VMAT2 sense probe as negative control shows the absence of labeling (B).

(C, D) Immunohistochemistry, paraffin-embedded sections. High power bright-field magnification showing VMAT2 expression in a perivascular mast cell infiltrate (C). The neoplastic mast cells lack VMAT1 expression (D).

Scale bars = 100 μ m in A, B, 50 μ m in C, D

Figure 8. Expression of VMAT2 in patients with systemic mastocytosis

(A-C) Immunohistochemistry for VMAT2 in bone marrow specimens of patients with ISM (A) and MCL (B) and in a liver specimen from a patient with ASM (C) revealing strong expression of VMAT2 in the neoplastic mast cell infiltrates.

(D-G) A case of MCL with infiltration of the pancreas revealing numerous inflammatory cells surrounding the ducts (D). The high power magnification shows that they contain very few Giemsa-positive granules (E). The corresponding confocal laser scanning double fluorescence microscopy reveals full coexpression of VMAT2 (F) and tryptase (G), confirming that the cells are mast cells.

Scale bars = 20 μ m in A-D, 20 μ m in E, 25 μ m in F

Figure 1

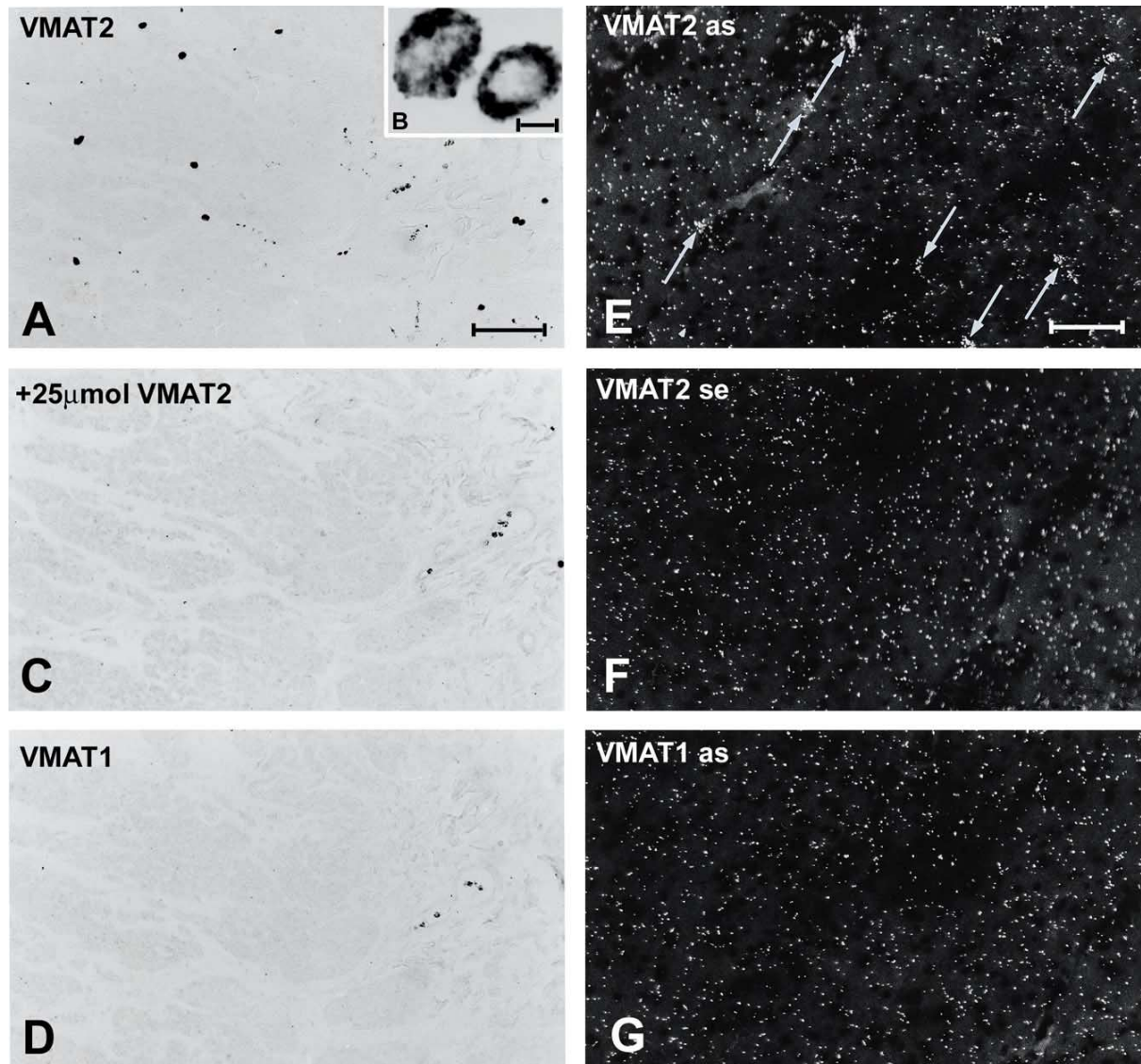


Figure 2

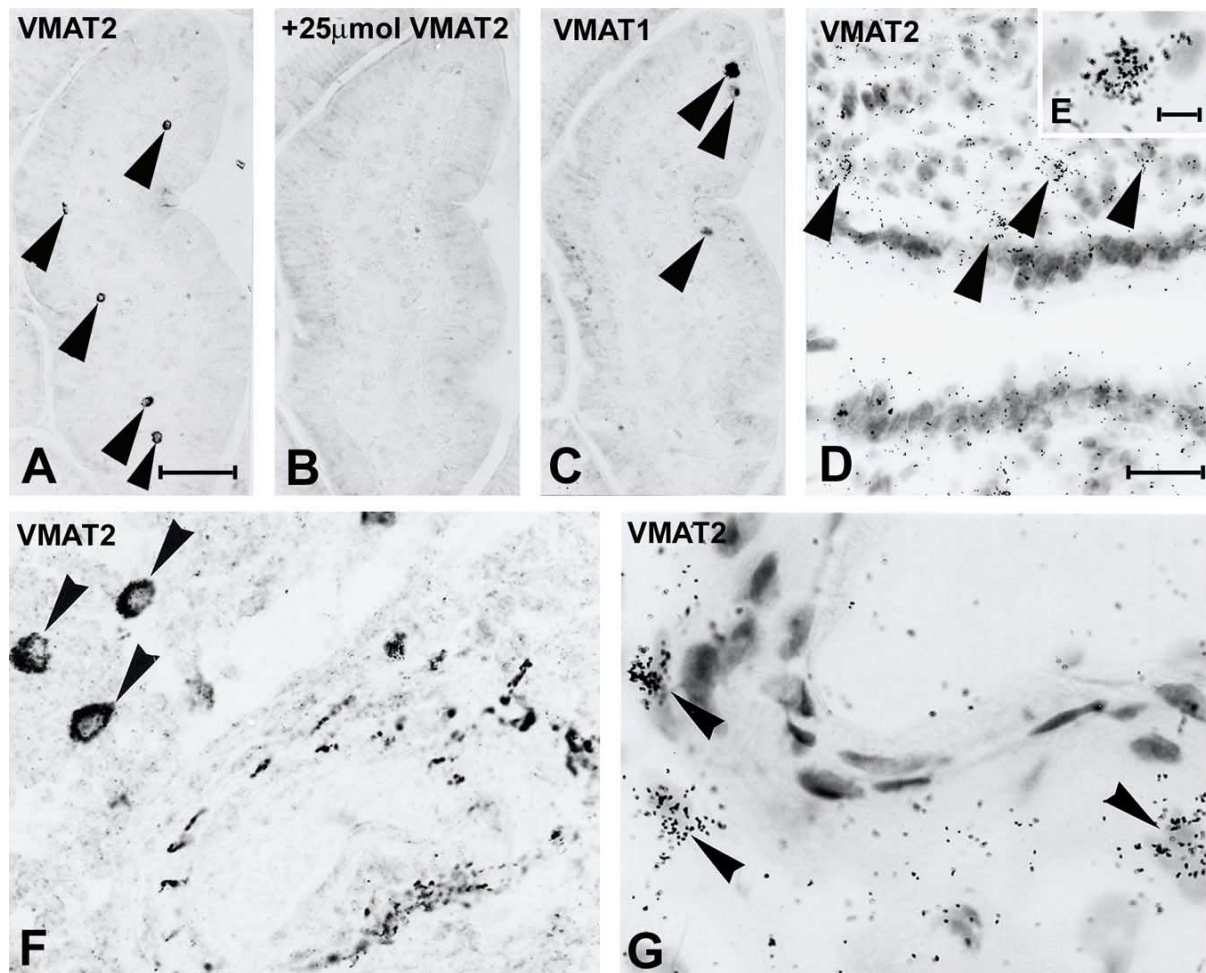


Figure 3

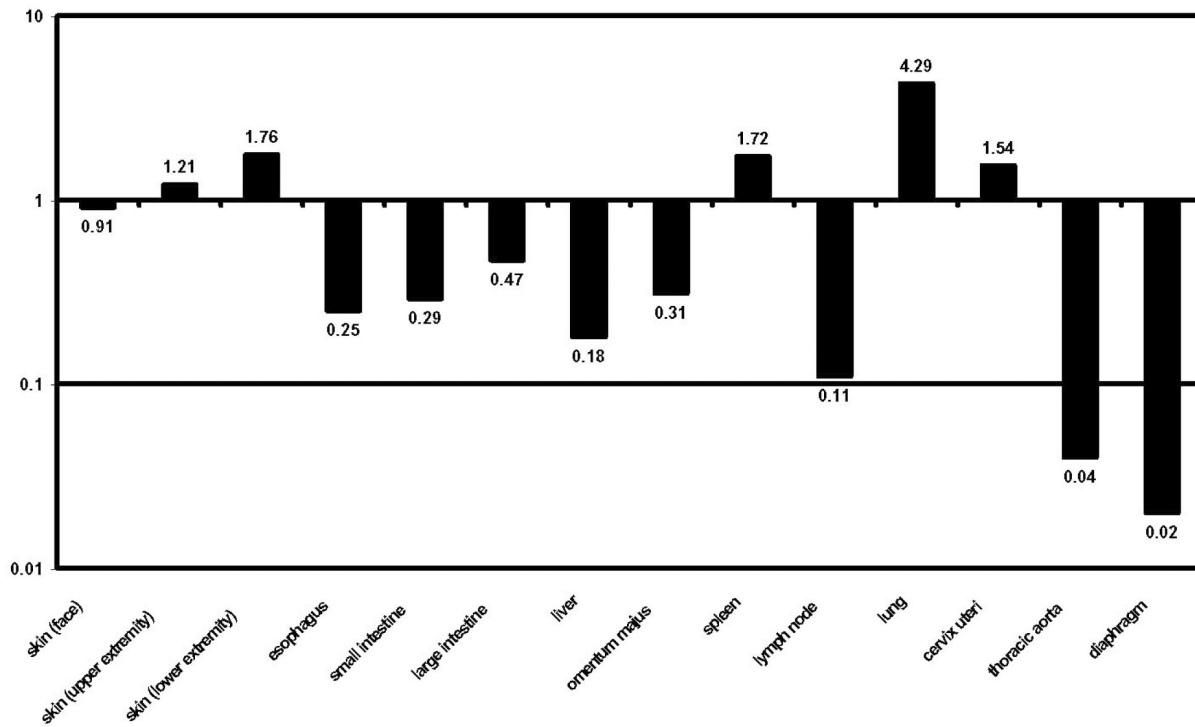


Figure 4

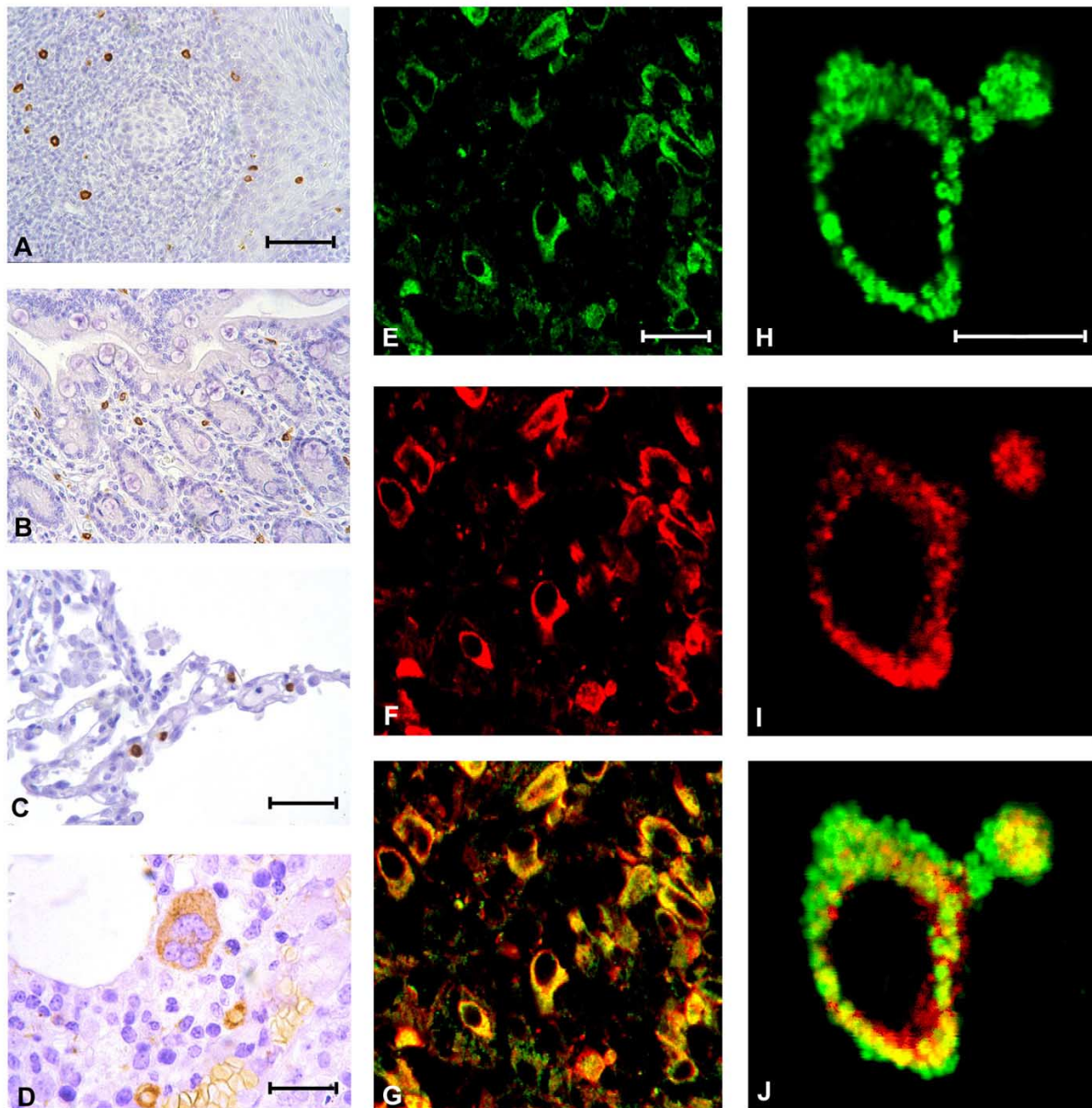


Figure 5

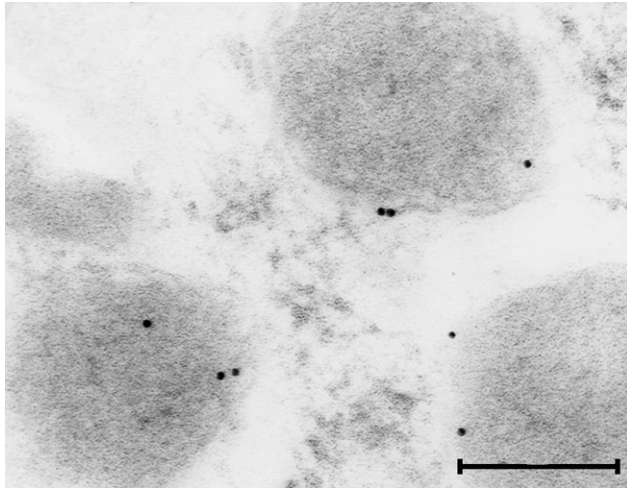


Figure 6

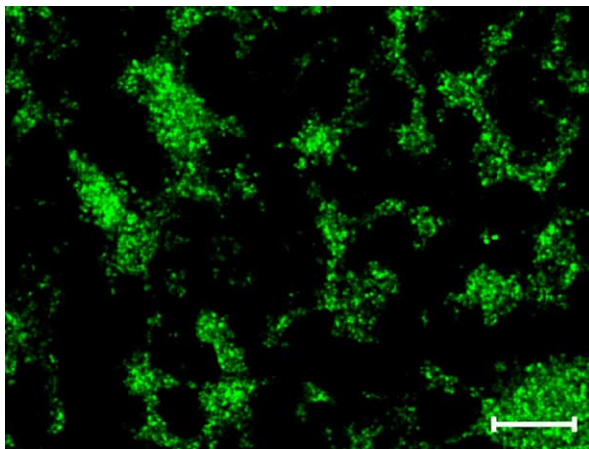


Figure 7

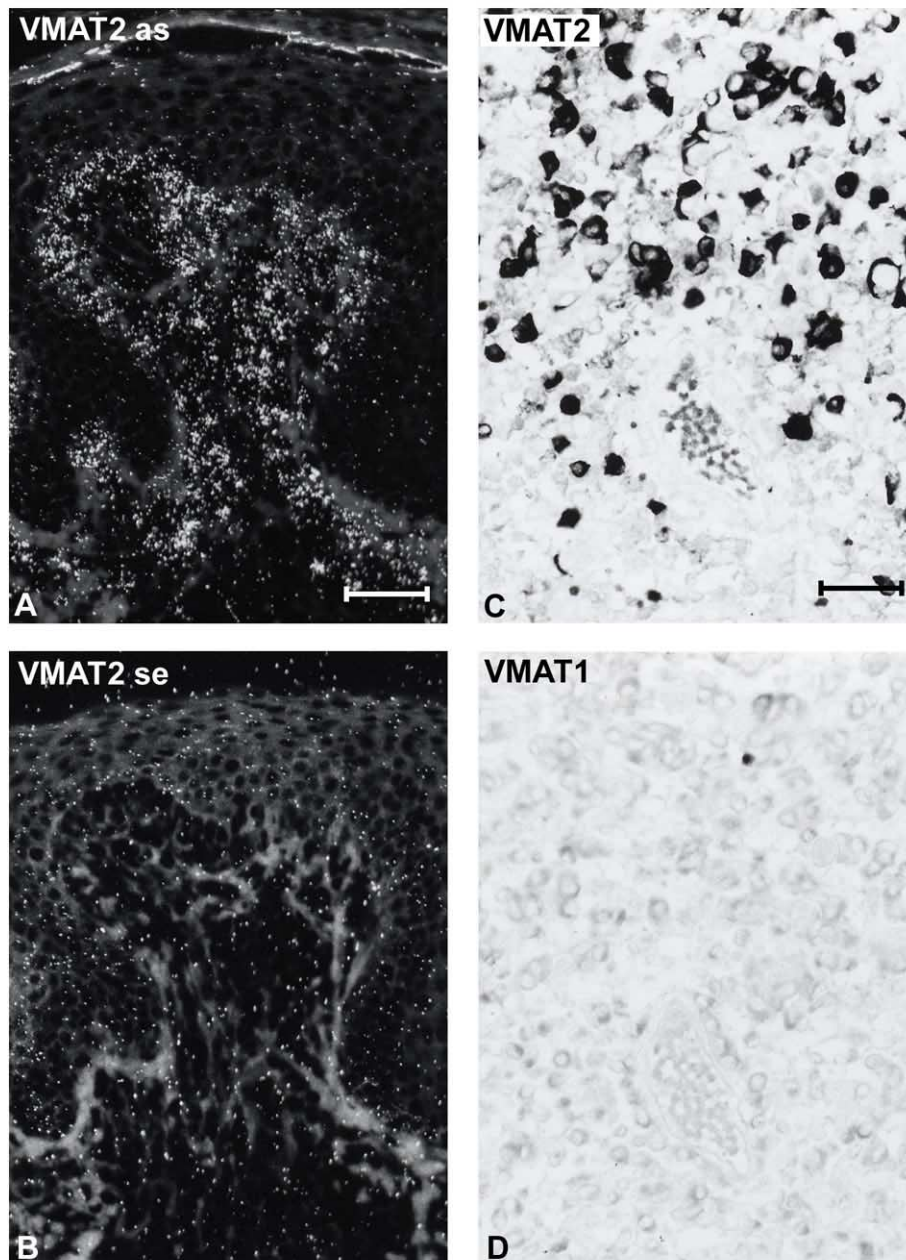


Figure 8

